Mechanical and Physical Characteristics of Cellulose-Fiber-Filled Polyacetal Composites

Kuniaki Kawaguchi,[1] Kazuhiro Mizuguchi,[1] Katsutoshi Suzuki,[1] Hideaki Sakamoto,[2] Toshio Oguni[2]

[1]*Research and Development Center, Polyplastics Company, Limited, 973, Miyajima, Fuji, Shizuoka, 416-8533 Japan*
[2]*Technical Development Center, Daicel Polymer, Limited, 12, Fuji-Cho, Hirohata-Ku, Himeji, Hyogo, 671-1123 Japan*

Received 2 October 2009; accepted 24 February 2010
DOI 10.1002/app.32338
Published online 8 June 2010 in Wiley InterScience (www.interscience.wiley.com).

ABSTRACT: We investigated the mechanical and physical characteristics of composites composed of polyacetal [alternatively called *polyoxymethylene* (POM)] and cellulose fiber (CelF) derived from wood pulp [10–52 wt % (9.3–50.1 vol %)] without any fiber surface treatment. The modulus, deflection temperature under load, and thermal conduction coefficient of the POM/CelF composites were effectively enhanced with increasing CelF content, and the composites had an advantage of specific modulus compared to glass fiber (GF)-filled POM. The flexural modulus of POM/CelF 40 wt % (38.2 vol %) was measured to be about 6 GPa, which was comparable to that of POM/GF 20 wt % (12.1 vol %). In the composites, the CelFs were distributed randomly as monofilaments, and the debonding of the interface between the fibers and POM matrices in the fracture faces was confirmed as less by scanning electron microscopy observation. The POM/CelF composites possessed lower specific wear rates than the POM/GF composites, and they had damping behaviors near that of neat POM. No clear dependence of the melt flow index of the base POM on these characteristics was observed, except on Charpy impact strength. The composites studied here were unique in their performance and ability to be designed in accordance with specific demands, and they could be potential replacements for mineral-filled and GF-filled POM composites. © 2010 Wiley Periodicals, Inc. J Appl Polym Sci 118: 1910–1920, 2010

Key words: composites; fibers; interfaces; mechanical properties; plastics

INTRODUCTION

Recently, the importance of the response to resources and environmental issues has been recognized in our society. There is a growing movement of minimizing our environmental footprint at every stage of the life cycle. As a valid response for minimizing the environmental impact of polymer and polymer composite production, there has been increased interest in composites made of versatile plastics and natural fibers.[1] Natural fibers, such as kenaf, hemp, flax, jute, sisal, bamboo, and wood, offer benefits such as reductions in weight, low ash, CO_2 neutrality, and less reliance on oil sources. Natural-fiber composites with versatile thermoplastic matrices, such as polyolefin and biobased polymers, have been researched, developed, and embraced for automotive and electrical & electronics parts.[2,3]

The use of natural fibers in engineering plastics has also been studied from the aspects of the high melting temperature (T_m) of these polymers and the possibility of the degradation of the natural fibers. It was demonstrated that the engineering plastics polyamide 6, polyamide 66, poly(butylene terephthalate), and polyketone could be reinforced with cellulose fiber (CelF) with a low-temperature processing or chill processing method with a twin-screw extruder to produce composites with promising structural applications.[4–7] It was also reported that polyamide 6/sugarcane–bagasse blends could be processed without much deterioration in the thermal properties when they were treated under low shear rates.[8] As for the use of solvent, the blend of cellulose with PA prepared by a solution–coagulation method was reported.[9–12] However, these engineering plastics with high T_m are basically at a disadvantage because of the high processing temperature required for the practical processing, namely, injection and other moldings, of composites.

Polyacetal [i.e., polyoxymethylene (POM)] is a major engineering thermoplastic that is widely used in automotive, electrical, electronics, and many industrial fields. It has been about half a century since the commercialization of POM began, and still, POM occupies an important position in society. This is due to its outstanding and well-balanced properties and because no other products can be substituted for POM in some application fields. It is

Correspondence to: K. Kawaguchi (kuniaki.kawaguchi@polyplastics.com).

expected that the development of high-value-added materials will be strongly required to distinguish them from existing POM materials.

In the case of POM, its glass fiber (GF)-filled composites and neat POM have also been used in many industrial fields.[13] Several research groups have investigated the preparation and properties of GF-filled POM from the theoretical and experimental points of view, including processing, fiber orientation, and composite properties.[14–24] On the other hand, surprisingly, there have been few reports of natural-fiber-filled POM composites, despite the lower T_m and processing temperature of POM compared to other engineering plastics; namely, T_m of the POM copolymer is about 165°C.

For example, POM/fique fiber composites were evaluated for the possibility of using fique fibers obtained from leaves to reinforce of POM.[25] However, many areas of research regarding the mechanical and physical characteristics of POM/natural-fiber composites are still undeveloped and could be developed for future technological progress.

Among thermoplastics, POM has the most exceptional friction and wear properties and exhibits superior tribological characteristics over extended use. In addition, it is generally self-lubricating and is used widely in nonlubricated components. In the case of POM/natural-material composites, reports on the friction and wear properties are scare, although there is increasing interest in the tribology of natural-fiber polymer composites.[26] The tribological characteristics of POM composites filled with low-density polyethylene and rice husk flour were reported as a three-component system;[27] however, the influence of natural fibers themselves in POM composites and, also, the differences compared to POM/GF composites have not been clear.

Moreover, vibration damping is becoming increasingly important for vibration control in advanced engineering systems, and polymer composites have generated increased interest in the development of damped structural materials.[28]

In this study, we investigated composites composed of POM and CelF as biobased and high-value-added engineering plastics and focused on the mechanical characteristics, tribological characteristics, damping characteristics, and thermal conduction characteristics of the composites as engineering plastics materials. Moreover, we discuss the dependence of the CelF content and melt flow index (MFI) of the base POM on these characteristics.

The degradation of natural fibers leads to poor organoleptic properties, such as odor and color, and also deterioration of their mechanical characteristics. The low-temperature degradation process in natural fibers associated with the degradation of hemicellulose and lignin is responsible for UV degradation and discoloration.[1] Therefore, we used wood pulp as a natural fiber in the composites when considering the high purity of CelF and the quality and accuracy of the composites.

EXPERIMENTAL

Preparation

CelF (virgin wood pulp supplied by Nippon Paper Group, Inc., Tokyo, Japan), which was received with no surface treatment, was dispersed in POM (Polyplastics Co., Ltd., Shizuoka, Japan; MFI = 9, 27, and 45 g/10 min) in a mixer below 200°C, and then, the POM/CelF composite materials [CelF content: 10–52 wt % (9.3–50.1 vol %)] were prepared with an extruder and chopped to form pellets. The composites obtained are listed in Table I, together with the data of specific gravity measured by a water substitution method at room temperature. The specific gravity of neat POM was measured to be 1.41, and that of CelF in the composites was calculated to be 1.52.

As for references, POM (MFI = 9 g/10 min)/GF (E-glass) [10 wt % (5.8 vol %), specific gravity = 1.46] and POM (MFI = 9 g/10 min)/GF [20 wt % (12.1 vol %), specific gravity =1.54] composites (prepared by Polyplastics Co., Ltd.) were also evaluated.

Specimens (4 mm thick) were injection-molded with a ROBOSHOT S2000i100B (Fanuc, Ltd., Yamanashi, Japan) according to ISO 527-1,2, ISO 178, ISO-179/1eA, and ISO 75-1,2. Specimens conforming to JIS K7218 were injection-molded with a Toshiba IS30FP (Tokyo, Japan). The cylinder nozzle temperature and molding temperature for all specimens were 200 and 90°C, respectively.

Morphology observation

Polarized light microscopy (PLM) observation was performed with an Olympus Corp. BX51 microscope (Tokyo, Japan) at room temperature. Specimens were prepared by the direct pressing of each sample once between two glass slides without a spacer in a molten state (200°C, 1 min) and then rapidly cooled to room temperature.

Scanning electron microscopy (SEM) observation was performed on a Hitachi, Ltd. S-4700 instrument (Tokyo, Japan) at room temperature with an acceleration voltage of 5 kV. The fractured surfaces of the tensile specimens ion-sputtered with platinum and palladium in a vacuum were used in the observation.

Crystallization and melting behavior

Differential scanning calorimetry measurements were performed on a PerkinElmer Japan Co., Ltd.,

TABLE I
List of Neat POM and the POM/CelF Composites

Sample	MFI of POM (g/10 min)	Weight fraction of CelF (%)	Volume fraction of CelF (%)	Specific gravity
POM (MFI = 9)	9	0	0	1.41
POM (MFI = 9)/CelF (10 wt %)	9	10	9.3	1.42
POM (MFI = 9)/CelF (20 wt %)	9	20	18.8	1.43
POM (MFI = 27)/CelF (20 wt %)	27	20	18.8	1.43
POM (MFI = 27)/CelF (30 wt %)	27	30	28.4	1.44
POM (MFI = 27)/CelF (40 wt %)	27	40	38.2	1.45
POM (MFI = 45)/CelF (30 wt %)	45	30	28.4	1.44
POM (MFI = 45)/CelF (40 wt %)	45	40	38.2	1.46
POM (MFI = 45)/CelF (52 wt %)	45	52	50.1	1.47

DSC-7 instrument (Kanagawa, Japan). The samples were held at 200°C for 1 min to remove any thermal history and cooled to 100°C at 10°C/min to observe the crystallization temperature [T_c (°C)] and the normalized heat of crystallization as POM fraction [ΔH_c (J/g of POM)]; then, they were heated to 200°C at 10°C/min to observe T_m (°C), and the normalized heat of fusion as POM fraction [ΔH_m (J/g of POM)] was observed. All measurements were performed under a nitrogen atmosphere. The instrument was calibrated with both indium and benzene.

Mechanical characteristics

Tensile strength (neat POM at yield, composites at break) and elongation (at break) were measured according to ISO 527-1,2. The flexural strength and modulus were measured according to ISO 178. An Autograph (Shimadzu Corp., Kyoto, Japan) was used for tensile tests with a crosshead speed of 50 mm/min and for flexural tests with a crosshead speed of 2 mm/min, respectively. The tests were performed at 23°C and 50% relative humidity (RH), and specimens were kept under the same conditions for more than 48 h before the tests. Five specimens of each sample were used for tensile and flexural tests, and the average values were reported.

Charpy impact strength tests were carried out according to ISO-179/1eA. The specimens molded with an injection-molding machine were made at a 45° notch. The tests were performed at 23°C and 50% RH, and the specimens were kept under the same conditions for more than 48 h before the tests. The impact strength was measured with an impact tester (Yasuda Seiki Seisakusho, Ltd., Hyogo, Japan) at room temperature. Five specimens of each sample were tested, and the average values were reported.

Deflection temperature under load (DTUL) was evaluated according to ISO 75-1,2 with a Toyoseiki Seisaku-Sho, Ltd. HDT & VSPT tester (Tokyo, Japan). A constant load (1.8 MPa) was applied at the center of a three-point bending specimen (4 mm thick) and heated at a rate of 2°C/min from 30°C. The temperature at which the specimen deflected by 0.34 mm under the application of a load was measured. Three specimens of each sample were tested, and the average values were reported.

MFIs of neat POMs were measured at 190°C with a load of 2.16 kgf according to ASTM D 1238 on a melt indexer (Takara Kogyo Co., Ltd., Tokyo, Japan).

Damping characteristics

The frequency dependence of the loss factor was investigated according to the JIS G0602 method (mechanical impedance method) on the basis of the steady vibration of the central support of the specimens (4 mm thick tensile specimens). The loss factor of each vibration mode (first, second, and third) for a frequency response function was calculated by a half-width method with a multipurpose CF-5220 FFT analyzer (Ono Sokki Co., Ltd., Kanagawa, Japan). The neat POM and composite materials were subjected to observation of the relationship between resonance frequency (Hz) at each vibration mode and loss factor at room temperature.

Thermal conduction characteristics

The thermal conductivity was evaluated by a hot-disk method with a TPA-501 thermal conductivity meter (Kyoto Electronics Manufacturing Co., Ltd., Kyoto, Japan). In this method, the hot-disk sensor consisted of an electrically conducting pattern in the shape of a double spiral that was laminated between two thin sheets of insulating material, and it was used both as a heat source and as a dynamic temperature sensor. The tests were performed at room temperature, and specimens were kept at 23°C and 50% RH for more than 24 h before the tests. The neat POM and composite materials (adjusted to a thickness of 6 mm) were subjected to a temperature rise, and an unsteady heat conduction equation was solved with the assumption that the hot disk was in an infinite medium, as follows:

$$\Delta T_{(\tau)} = \frac{P_0}{\pi^{3/2} r \lambda} D_{(\tau)} \quad (1)$$

$$\tau = \sqrt{\alpha t / r^2} \quad (2)$$

where $\Delta T_{(\tau)}$ is the temperature of the sensor (K), P_0 is the heat quantity generated in the heater (W), $D_{(\tau)}$ is the function of dimensionless τ, r is the radius of the hot disk (m), λ is the thermal conduction coefficient (W/m K), α is the thermal diffusivity (m^2/s), and t is the measurement time (s).

Tribological characteristics

The wear-resistance properties were evaluated according to JIS K7218 (specified method to standard A) with an Orientec Co., Ltd., EFM-III-EN (Tokyo, Japan). The wear-resistance tests between carbon steel S45C and the POM materials (the neat POM and POM/CelF composites) were carried out with ring-on-ring-type (hollow-cylinder-type) specimens, and the specific wear rates were measured both for the S45C part (rotational side) and the POM part (fixed side). The test conditions were as follows: test environment: 23°C in the air, contact area: 2.0 cm^2, surface pressure: 0.98 MPa, velocity: 17.9 cm/s, and time: 24 h.

RESULTS AND DISCUSSION

Morphology and thermal behavior of the POM/CelF composites

PLM and SEM observations were performed to investigate the morphology of the POM/CelF composites. Figure 1 shows the polarized light micrographs of the POM (MFI = 27 g/10 min)/CelF 30 wt % (28.4 vol %), POM (MFI = 45 g/10 min)/CelF 30 wt % (28.4 vol %), and POM (MFI = 45 g/10 min)/CelF 40 wt % (38.2 vol %) composites rapidly cooled to room temperature from 200°C. The CelFs were observed along the in-plane direction of the specimens because the specimens were prepared by direct pressure between two glass slides in a molten state. In the composites, each fiber was distributed randomly in the POM matrices covered with spherulites and was twisted and turned upon other fibers. The fibers were observed to be in a ribbon form, and the cross section of the fibers seemed to be flat. In the micrographs, there was little or no difference in the dispersion of the fibers, although the MFI values of the base POM or the CelF content were different. The results indicate that the wood pulp used in this study was well dispersed as monofilaments in the POM matrices.

Figure 2 shows the SEM micrographs of the tensile fractured surfaces of the specimens [the POM (MFI = 27 g/10 min)/CelF 30 wt % (28.4 vol %) and POM (MFI = 45 g/10 min)/CelF 52 wt % (50.1 vol %) composites]. The monofilaments of the CelFs distributed in the POM matrices were observed in each micrograph, and the most CelFs seemed to be broken in the composites during tensile fracture. The debonding of the interface between the CelFs and the POM matrices was less confirmed, and the

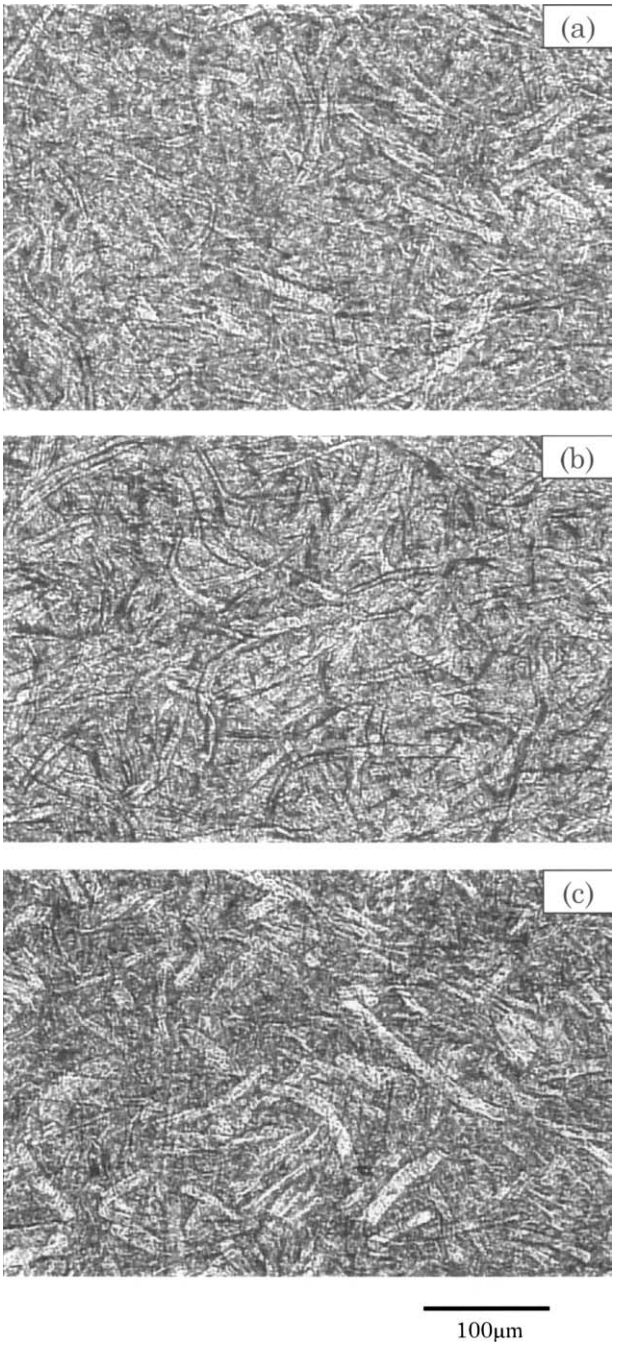

Figure 1 Polarized light micrograph of specimens rapidly cooled to room temperature from 200°C: (a) POM (MFI = 27 g/10 min)/CelF 30 wt % (28.4 vol %), (b) POM (MFI = 45 g/10 min)/CelF 30 wt % (28.4 vol %), and (c) POM (MFI = 45 g/10 min)/CelF 40 wt % (38.2 vol %).

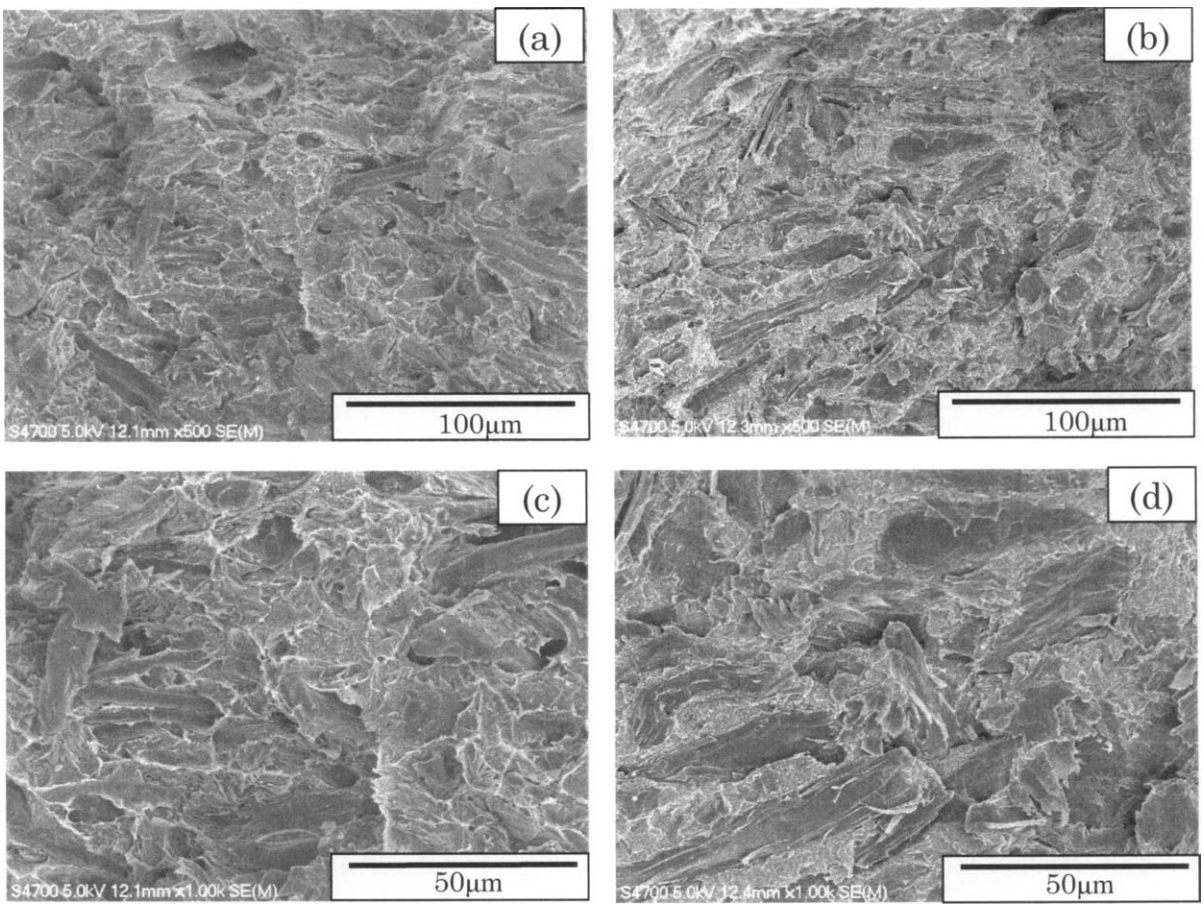

Figure 2 SEM micrographs of the tensile fractured surfaces of the specimens: (a) POM (MFI = 27 g/10 min)/CelF 30 wt % (28.4 vol %) and (b) POM (MFI = 45 g/10 min)/CelF 52 wt % (50.1 vol %) and magnified photographs of (c) a and (d) b.

periphery of the CelFs in the POM matrices appeared to be complicated [see the magnified photographs in Fig. 2(c,d)]. These results of SEM observation indicate good interfacial adhesion between the CelFs (which received no surface treatment) and the POM matrices during the tensile fracture process. The interface between the fibers and polymer matrices was very closely linked to the mechanical properties of the composite materials and to the intrinsic characteristics of the matrices and the fibers because it should have allowed for an efficient transfer of the mechanical stresses within the composite materials. Therefore, the results support the high stiffness and modulus properties of the composites, as mentioned in the next section. CelFs tend to aggregate and do not disperse well in hydrophobic polymer matrices, such as polyethylene and polypropylene, and thus, pose difficulties in the achievement of a uniform distribution of fibers in the matrices.[1] In contrast, in the case of the POM/CelF composites, the fibers dispersed well in the polymer matrices, probably because of the good compatibility derived from the similarity in the chemical structures between the fibers and the matrices, especially in the oxymethylene backbone and hydroxyl moieties.

Table II shows the differential scanning calorimetry analytical results of the samples: T_c, T_m, ΔH_c, ΔH_m, and the degree of crystallinity (X_c). X_c is given by the following equation:

$$X_c\ (\%) = \frac{\Delta H_m}{\Delta H_m^0} \times 100 \qquad (3)$$

where ΔH_m^0 is the enthalpy of fusion per gram for 100% crystalline POM, which was assumed to be 248.3 J/g (59.3 cal/g).[29] The T_c and T_m values of the POM/CelF composites shifted to slightly higher temperatures with the addition of CelFs. The results indicate that the CelFs gave a nucleating effect to the POM matrices, but the effect was not too large. On the other hand, most of the ΔH_c, ΔH_m, and X_c values of the POM/CelF composites were measured to be the same or less when compared to those of the neat POM. The mechanical strength of semicrystalline polymers correlates to X_c. Therefore, the results suggest that the CelFs did not contribute with respect to the enhancement of crystallinity to the stiffness and

TABLE II
Crystallization and Melting Behavior of Neat POM and the POM/CelF Composites

Sample	T_c (°C)	ΔH_c (J/g of POM)	T_m (°C)	ΔH_m (J/g of POM)	X_c (%)
POM (MFI = 9)	143.1	141.9	163.7	148.7	59.9
POM (MFI = 9)/CelF (20 wt %)	143.5	128.0	165.2	137.3	55.3
POM (MFI = 27)/CelF (20 wt %)	143.8	128.9	164.2	138.4	55.7
POM (MFI = 27)/CelF (30 wt %)	144.7	137.5	164.9	141.4	57.0
POM (MFI = 27)/CelF (40 wt %)	143.8	141.7	164.7	148.7	59.9
POM (MFI = 45)/CelF (30 wt %)	144.7	140.3	164.4	143.9	58.0
POM (MFI = 45)/CelF (40 wt %)	145.2	142.2	165.0	147.4	59.4
POM (MFI = 45)/CelF (52 wt %)	146.0	143.3	165.0	144.9	58.4

modulus improvement of the POM/CelF composites.

Mechanical characteristics of the POM/CelF composites

The tensile properties, flexural properties, DTUL, and impact properties of the neat POM and composites were investigated. Their stress–strain curves of the tensile tests are shown in Figure 3. Figure 4 shows the tensile strength and elongation of the neat POM and the composites versus the CelF content (vol %), respectively. The tensile modulus (initial slope of the stress–strain curve) increased with increasing CelF content, as shown in Figure 3. The stress–strain curves and the morphology observed in the SEM micrograph (Fig. 2) suggested that the CelFs worked to transfer an efficient tensile stress from the POM matrices to the fibers. The tensile strength of the POM/CelF composites decreased at lower CelF contents, and afterward, when the fiber content was higher than 10 wt %, it increased with the fiber content (Fig. 4). In the case of lower CelF contents, the slopes of the stress–strain curves became gradual as the strain increased, which resulted in a lower tensile strength at break of the composites. On the other hand, in the case of higher CelF contents, the higher modulus of the composites led directly to a higher tensile strength at break. The MFI of the base POM had substantially less dependence on the tensile modulus and strength of the composites. Figure 5 shows the CelF content (vol %) dependence of the flexural modulus and strength. The flexural modulus increased with increasing CelF content and was given an approximately linear relationship, regardless of the MFI value of the base POM. The results indicate that the flexural modulus was more influenced by the CelF content. The flexural modulus of the POM/CelF 40 wt % (38.2 vol %) composite was around 6 GPa, and this was comparable to the value of the POM/GF 20 wt % (12.1 vol %) composite. The flexural strength of the POM/CelF composites kept an almost constant value at lower CelF contents, and afterward, when the fiber content was higher than 10 wt %, it increased with the fiber content. This also suggested that the CelFs could work to transfer an efficient flexural stress from the POM matrices to the fiber.

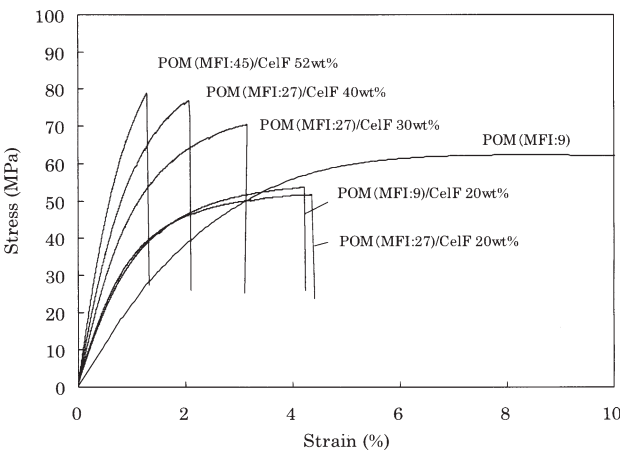

Figure 3 Stress–strain curves of neat POM and the POM/CelF composites. The tensile elongation of neat POM was measured to be 30.4%, and the data is shown up to 10% of tensile strength.

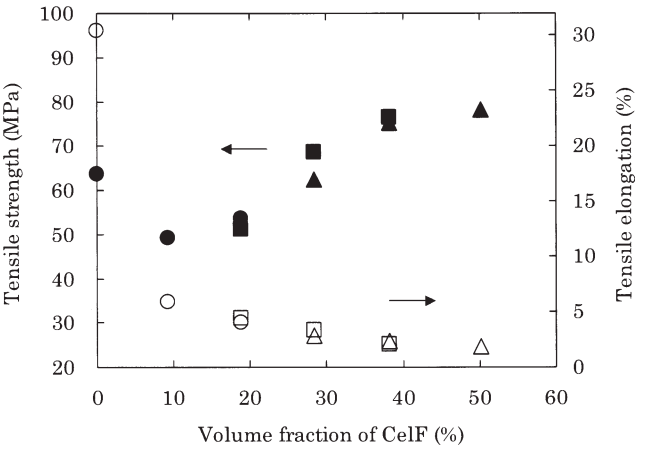

Figure 4 Tensile strength (closed symbols) and elongation (open symbols) of neat POM and the POM/CelF composites with various CelF contents and MFIs of the base POM [9 g/10 min (circle), 27 g/10 min (square), and 45 g/10 min (triangle)].

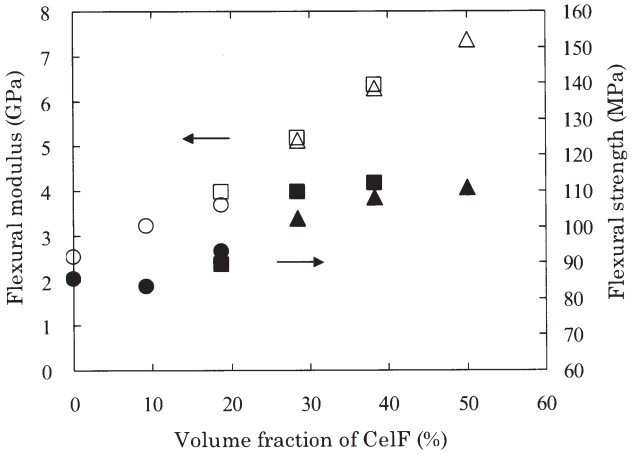

Figure 5 Flexural modulus (open symbols) and flexural strength (closed symbols)of neat POM and the POM/CelF composites with various CelF contents and MFIs of the base POM [9 g/10 min (circle), 27 g/10 min (square), and 45 g/10 min (triangle)].

The correlation between the flexural modulus and the specific gravity of the POM/CelF composites is shown in Figure 6, together with the data for the POM/GF composites. Least-squares fitted lines are inserted in the figure for better visualization. At the same specific gravity, the flexural modulus of the POM/CelF composites was higher than those of the POM/GF composites. For example, the specific gravity of POM/CelF 40 wt % (38.2 vol %) was measured to be 1.45–1.46, whereas that of POM/GF 20 wt % (12.1 vol %) was 1.54. This indicated that CelFs is a promising filler for fiber-reinforced POMs to reduce product weight and maintain mechanical characteristics. Figure 7 shows the relationship between DTUL and the CelF content (vol %). Dependence of the MFI of the base POM on the DTUL was not clearly observed. Similar to the flexural

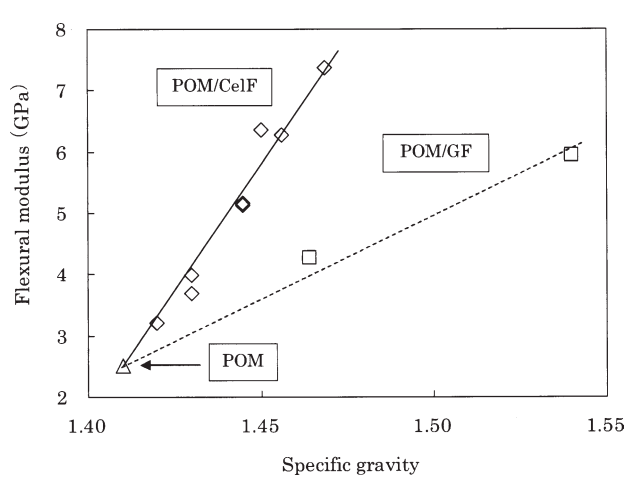

Figure 6 Correlation between the flexural modulus and specific gravity of neat POM, the POM/CelF composites, and the POM/GF composites.

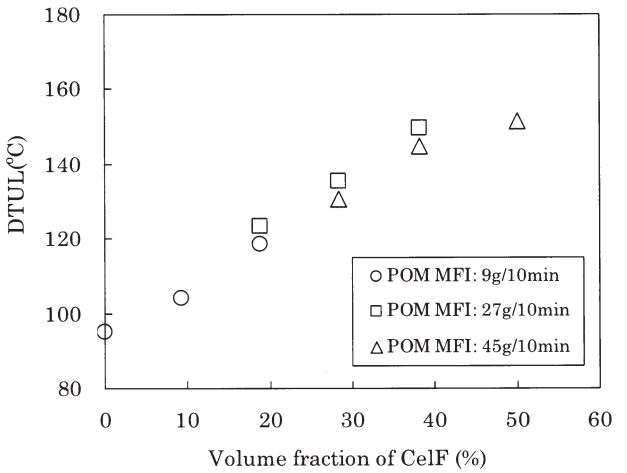

Figure 7 DTUL of neat POM and the POM/CelF composites with various CelF contents and MFIs of the base POM.

modulus, DTUL of the composites increased linearly with increasing CelF content, and then, a gradual increase was observed at higher fiber contents. Overall, the POM/CelF composites possessed a high modulus, stiffness, and DTUL properties without any fiber surface treatment, and they had a great advantage of specific modulus compared to mineral- and GF-reinforced POM composites.

The Charpy impact strength of the POM/CelF composites decreased compared to that of neat POM (Fig. 8). This was explained by the fact that the fiber created regions of stress concentrations that required less energy to elongate the crack propagation.[30,31] Also, the Charpy impact strength showed a decline with increasing MFI value of the POM matrices, as shown in Figure 8. There should have been an influence on the impact properties coming from the difference between the states of entanglement or

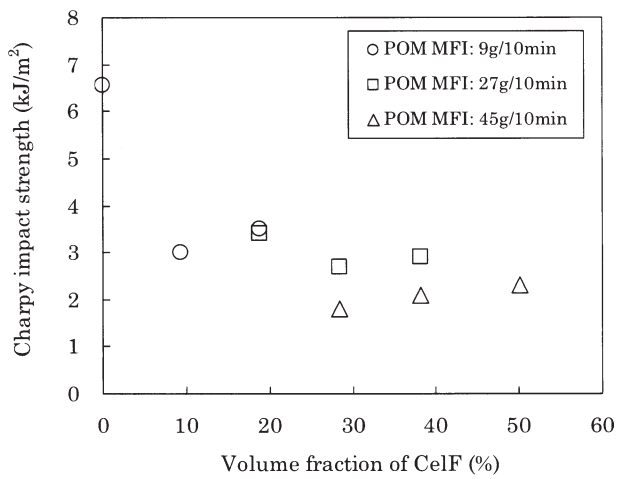

Figure 8 Charpy impact strength of neat POM and the POM/CelF composites with various CelF contents and MFIs of the base POM.

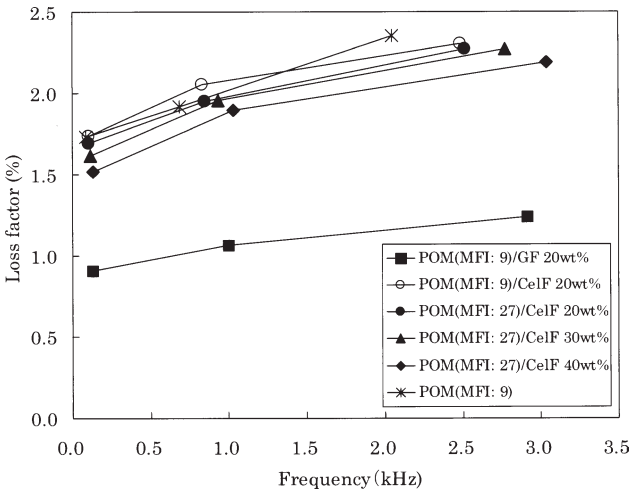

Figure 9 Frequency dependence of the loss factor of neat POM and the POM/CelF composites.

aggregation of the polymer chains caused by low-MFI POM and those caused by high-MFI POM. As shown in Figure 2(c), for the case of POM (MFI = 27 g/10 min)/CelF 30 wt % (28.4 vol %), the edge of the fracture matrix was more elongated, and the tensile fracture surface appeared to be more ductile. This also suggested MFI dependence on the fracture behavior of the composites. On the other hand, the mechanical characteristics of thermoplastic composites can be further improved by the improvement of the compatibility between the fiber and the matrices. The impact properties and the stiffness properties obtained here for the POM/CelF composites could be further optimized through the use of compatibilizers and coupling agents.

Damping characteristics of the POM/CelF composites

The damping characteristics of the neat POM and composites were investigated on the basis of the cantilever method (mechanical impedance method) specified by JIS G0602 and were subjected to observation of the relationship between the resonance frequency and the loss factor. Figure 9 shows the frequency dependence of the loss factor of the neat POM and the composites. The plots are lined in the figure for better visualization. The loss factor, which was obtained from each vibration mode (first, second, and third) for the frequency response function, increased with increasing resonance frequency in the range 0–3 kHz, and the trend was substantially similar for all of the samples.

The POM/GF composites had a lower loss factor over the range of resonance frequencies. By contrast, the POM/CelF composites had a higher value, and these values were close to the loss factor of the neat POM, even with the higher CelF content. For example, the loss factor of the POM/CelF 40 wt % (38.2 vol %) composite at 1 kHz (second vibration mode) was about 78% higher compared to that of the POM/GF 20 wt % (12.1 vol %) composite. In addition, the loss factors of the POM/CelF composites with different base POMs were measured to be nearly the same. The results indicate that the difference of the fibers greatly influenced the loss factors of the composites, and the POM/CelF composites had better damping characteristics than the POM/GF composites. Some of the micromechanical-level geometric and material parameters can affect the damping of a composite system.[28] The damping of the POM/CelF composites could have been influenced by the characteristics of the CelFs, such as the modulus of the fibers. Further rheological analysis is necessary to clarify the effect of the CelFs on the damping of the composites. On the other hand, the results could give a model combination that could possess improved mechanical properties maintaining better damping characteristics, and the composites seemed to be available for vibration control, such as noise and vibrational absorption.

Thermal conduction characteristics of the POM/CelF composites

The thermal conduction characteristics of the neat POM and composites were evaluated by the hot-disk method. Figure 10 shows the relationship between the thermal conduction coefficient and the CelF content (vol %) for the POM/CelF composites with each MFI of the base POM. The thermal conduction coefficient of the neat POM and POM/CelF 52 wt % (50.1 vol %) were measured to be 0.39 and 0.48 W m^{-1} K^{-1}, respectively. The POM/CelF

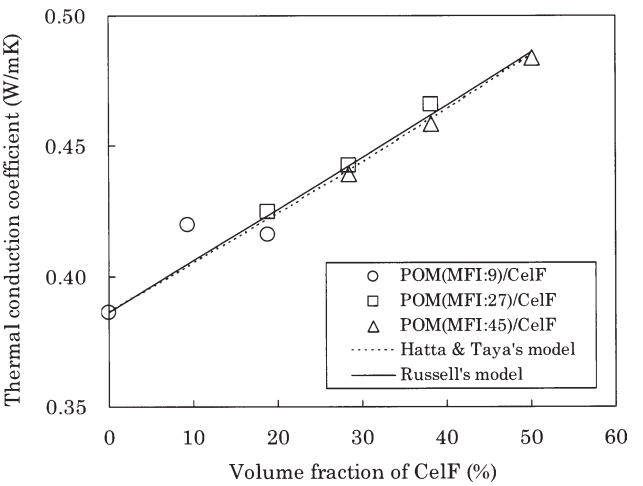

Figure 10 Thermal conduction coefficient of neat POM and the POM/CelF composites with various CelF contents and MFIs of the base POM: measured data and calculated values based on Hatta and Taya's model and Russell's model.

composites studied here had almost better thermal conductivity compared to the POM/GF 20 wt % (12.1 vol %) composite, whose thermal conductivity was measured to be 0.41 W m^{-1} K^{-1}. It was clearly observed that incorporation of the CelFs in the POM matrices resulted in an increase in the thermal conductivity, which indicated that the nature of the monofilaments of the CelFs in the POM composites played an important role in generating these thermal conduction characteristics.

Several prediction models for the thermal conductivity of composites have been proposed.[32–35] In this article, we applied Hatta and Taya's model[35] (a simplified version[36]) and Russell's model[33] to analyze the thermal conductivity of the POM/CelF composites. The equations are presented as follows:

$$\frac{\lambda_c}{\lambda_m} = 1 + \frac{V(\lambda_f - \lambda_m)[(\lambda_f - \lambda_m)1/2 + 3\lambda_m]}{\lambda_m(\lambda_f - \lambda_m)(3 - 2V)1/2 + 3(\lambda_m)^2} \quad (4)$$

$$\frac{\lambda_c}{\lambda_m} = \frac{V^{2/3} + \frac{\lambda_m}{\lambda_f}(1 - V^{2/3})}{V^{2/3} - V + \frac{\lambda_m}{\lambda_f}(1 - V^{2/3} + V)} \quad (5)$$

where λ_c is the thermal conduction coefficient of the composites (assumed to be the experimental value in this study); λ_m and λ_f are the thermal conduction coefficients of the matrix (neat POM) and the fibers, respectively; and V is the fiber volume fraction. As shown in Figure 10, both model equations successfully predicted the thermal conductivity of the POM/CelF composites regardless of the MFI value of the base POM. From both prediction models, the thermal conduction coefficient of the CelF in the composites was estimated to be 0.60 W m^{-1} K^{-1}, which was about 55% higher than that of the neat POM.

Natural-fiber materials are superior to insulation and are less thermally conductive;[37] however, as estimated, the monofilaments of CelFs possess excellent thermal conductivity. This can be explained by the fact that there is no or less of an air layer (hollow structure) around the periphery of the fibers in the composites, unlike other composites with such fillers such as bamboo and wood fibers. Shimazaki et al.[38] reported excellent thermal conductivity in cellulose nanofiber/epoxy resin nanocomposites. They suggested that phonon scattering in the cellulose nanofiber was small compared to that in the epoxy resin and indicated that a large amount of nanofibers could transport more phonons through the nanocomposites. Likewise, the monofilaments of the CelFs derived from wood pulp studied here, consisting of about 50–60% crystallized cellulose chains, functioned as efficient pathways of phonons in the POM/CelF composites and resulted in the higher thermal conduction coefficient of the composites.

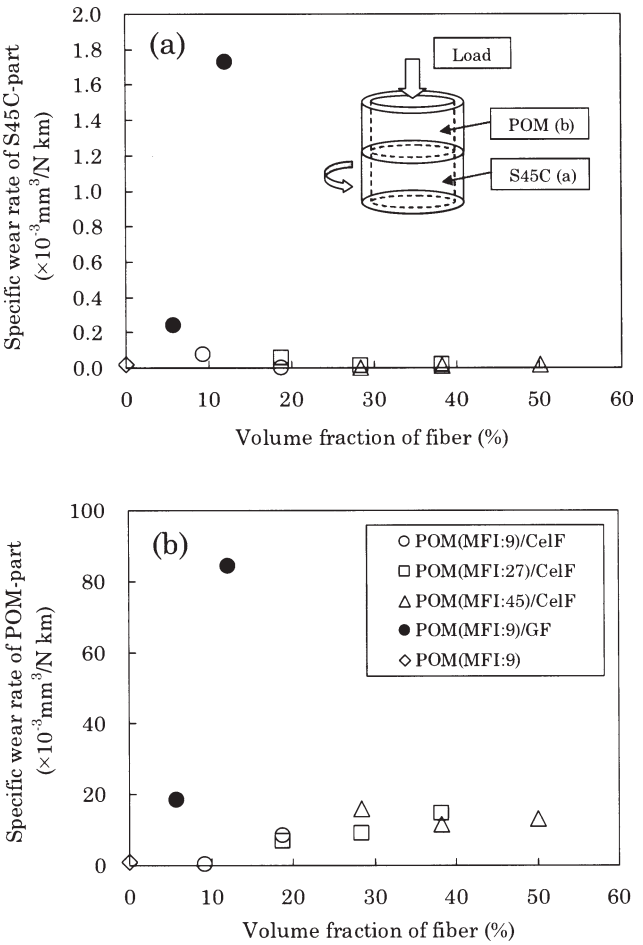

Figure 11 Specific wear rates of the (a) S45C part and (b) POM part for neat POM, the POM/CelF composites, and the POM/GF composites with various fiber contents and MFIs of the base POM. The ring-on-ring test pieces used in the test are illustrated in part a.

Tribological characteristics of the POM/CelF composites

The tribological characteristics of neat POM and the POM/CelF composites with each MFI of the base POM were investigated with a focus on the wear-resistance properties. The specific wear rates were measured both for the S45C part (rotational side) and the POM part (fixed side, the neat POM and POM/CelF composites), according to JIS K7218. Figure 11(a) shows the specific wear rate of the S45C part after the test. Dependence of the MFI of the base POM on the specific wear rate of the S45C part was not clearly observed. In the case of the neat POM, the measured value was 2.1×10^{-5} mm^3/N km. The POM/GF 20 wt % (12.1 vol %) composite showed a significantly higher rate, 1.7×10^{-3} mm^3/N km. In contrast, the POM/CelF composite materials had extremely lower rates compared to the POM/GF composites. For example, the specific wear rate of the S45C part for POM (MFI = 27 g/10 min)/CelF 20 wt % (18.8 vol %) was measured to be

5.9×10^{-5} mm^3/N km. The results indicate that the difference of the fibers greatly influenced the specific wear rate of the S45C part, and the CelFs caused lower surface damages of the S45C part. It is thought that the specific wear rate of the S45C part received the influence by the difference in the surface hardness of the fibers in the composites.

Figure 11(b) shows the specific wear rate of the POM part after the test. Dependence of the MFI of the base POM on the specific wear rate of the POM part was not clearly observed. In the case of the neat POM, the rate of the POM part was measured to be 8.9×10^{-4} mm^3/N km. The POM/GF 20 wt % (12.1 vol %) composite also showed a significantly higher rate, 8.4×10^{-2} mm^3/N km. On the other hand, the POM/CelF composites had lower rates of the POM part. For instance, the specific wear rate of the POM (MFI = 27 g/10 min)/CelF 20 wt % (18.8 vol %) composite was measured to be 6.8×10^{-3} mm^3/N km. With increasing CelF content (vol %), the specific wear rate of the POM part gradually increased; then, it remained at an almost constant value. Overall, the test results indicate that the CelFs could be a potential reinforcement for the POM composites, which had good tribological characteristics. In the case of natural-fiber-reinforced polyesters, a good degree of wear resistance was reported for sliding against stainless steel; this suggested that natural fibers contribute well to building up smooth protective layers at the interface.[39] We considered that the POM/CelF composites are also at an advantage in having protective layers, which minimize the surface damage of the composites. Interfacial adhesion between fibers and matrices is a crucial factor for the specific wear rate of composites.[26] The lower specific wear rate of the POM part in the composites could also have been due to better interfacial adhesion between the CelFs and POM matrices. Chand and Dwivedi,[40] on the other hand, reported that the specific wear rate of composites materials were influenced by the fiber arrangement and orientation for sisal fiber/epoxy composites. When fibers are aligned longitudinally (parallel) to the sliding direction, there is a maximum contact area during sliding, and therefore, severe damage is caused throughout the length of the fibers, which results in the removal of debris.[26] Detailed study is further necessary to determine the effect of fiber arrangement and orientation on the tribological characteristics of the POM/CelF composites and other properties through the analysis of flow behaviors in a mold.

CONCLUSIONS

The mechanical and physical characteristics of POM/CelF composites as biobased and high-value-added engineering plastics were investigated. The POM/CelF composites possessed high modulus, stiffness, and DTUL values, and they had an advantage of specific modulus compared to the GF-filled POM composites. The results of SEM observation indicate good interfacial adhesion between the monofilaments of the CelFs and the POM matrices during the fracture process. The POM/CelF composites possessed dumping characteristics near those of neat POM, and they had lower specific wear rates of the S45C part and POM part than the POM/GF composites, in addition to their high thermal conductivity. The MFI of the base POM had no clear dependence on these characteristics, except on the Charpy impact strength. The composites studied here were unique in their performance and ability to be designed in accordance with specific demands. Further research and application development with the unique balance of properties obtained by the combination of the CelFs and POM matrices are desired.

References

1. Nabi Saheb, D.; Jog, J. P. Adv Polym Tech 1999, 18, 351.
2. Holbery, J.; Houston, D. JOM 2006, 58, 80.
3. Iji, M.; Serizawa, S.; Inoue, K. Funct Mater 2004, 24, 66.
4. Sears, K.; Jacobson, R.; Caulfield, D.; Underwood, J. Presented at the Sixth International Conference on Woodfiber–Plastic Composites, Madison, Wisconsin, May 2001.
5. Jacobson, R.; Caulfield, D.; Sears, K.; Underwood, J. Presented at the Sixth International Conference on Woodfiber–Plastic Composites, Madison, Wisconsin, May 2001.
6. Caulfield, D.; Jacobson, R.; Sears, K.; Underwood, J. Presented at PPS-17, Montreal, Canada, May 2001.
7. Caulfield, D.; Jacobson, R.; Sears, K.; Underwood, J. Presented at the 2nd International Conference on Advance Engineered Wood Composites, Bethel, Maine, Aug 2001.
8. Dweiri, R.; Azhari, C. H. J Appl Polym Sci 2004, 92, 3744.
9. Nishio, Y.; Manley, R. S. J Polym Eng Sci 1990, 30, 71.
10. Garcia-Ramirez, M.; Cavaillé, J. Y.; Dupeyre, D.; Péguy, A. J Polym Sci Part B: Polym Phys 1994, 32, 1437.
11. Garcia-Ramirez, M.; Cavaillé, J. Y.; Dufresne, A.; Tékély, P. J Polym Sci Part B: Polym Phys 1995, 33, 2109.
12. Garcia-Ramirez, M.; Cavaillé, J. Y.; Dufresne, A.; Dupeyre, D. J Appl Polym Sci 1996, 59, 1995.
13. Barker, S. J.; Price, M. B. Polyacetals; The Plastics Institute: London, 1970; p 143.
14. Hardy, G. F.; Wagner, H. L. J Appl Polym Sci 1969, 13, 961.
15. Hardy, G. F. J Appl Polym Sci 1971, 15, 853.
16. Kastelic, J.; Hope, P.; Ward, I. M. Org Coat Plast Chem 1981, 44, 290.
17. Hope, P. S.; Richardson, A.; Ward, I. M. Polym Eng Sci 1982, 22, 307.
18. Curtis, A. C.; Hope, P. S.; Ward, I. M. Polym Compos 1982, 3, 138.
19. Hope, P. S.; Brew, B.; Ward, I. M. Plast Rubber Process Appl 1984, 4, 229.
20. Hine, P. J.; Duckett, R. A.; Ward, I. M. Composites 1993, 24, 643.
21. Hine, P. J.; Davidson, N.; Duckett, R. A.; Clarke, A. R.; Ward, I. M. Polym Compos 1996, 17, 720.
22. Hine, P. J.; Wire, S.; Duckett, R. A.; Ward, I. M. Polym Compos 1997, 18, 634.

23. Zachariev, G.; Rudolph, H. V.; Ivers, H. Compos A 2004, 35, 1119.
24. Kawaguchi, K.; Masuda, E.; Tajima, Y. J Appl Polym Sci 2008, 107, 667.
25. Gañán, P.; Mondragon, I. J Compos Mater 2005, 39, 633.
26. Chand, N.; Fahim, M. Tribology of Natural Fiber Polymer Composites; Woodhead: Cambridge, England, 2008.
27. Li, K.; Xiang, D.; Lei, X. J Appl Polym Sci 2008, 108, 2778.
28. Finegan, I. C.; Gibson, R. F. Compos Struct 1999, 44, 89.
29. Starkweather, H. W.; Boyd, R. H. J Phys Chem 1960, 64, 410.
30. Hunda, M. S.; Mohanty, A, K.; Drzal, L. T.; Schut, E.; Misra, M. J Mater Sci 2005, 40, 4221.
31. Pan, P.; Zhu, B.; Dong, T.; Serizawa, S.; Iji, M.; Inoue, Y. J Appl Polym Sci 2008, 107, 3512.
32. Bruggeman, D. A. G. Ann Phys 1935, 24, 636.
33. Russell, H. W. J Am Ceram Soc 1935, 18, 1.
34. Nielsen, L. E. Mechanical Properties of Polymer and Composites 2; Marcel Dekker: New York, 1974.
35. Hatta, H.; Taya, M. J Appl Phys 1985, 58, 2478.
36. Torres, F. G.; Flores, R.; Dienstmaier, J. F.; Quintana, O. A. Polym Polym Compos 2005, 13, 753.
37. Takagi, H.; Kako, S.; Kusano, K.; Ousaka, A. Adv Compos Mater 2007, 16, 377.
38. Shimazaki, Y.; Miyazaki, Y.; Takezawa, Y.; Nogi, M.; Abe, K.; Ifuku, S.; Yano, H. Biomacromolecules 2007, 8, 2976.
39. El-Tayeb, N. S. M. Proc Inst Mech Eng Part J: J Eng Tribol 2008, 222, 935.
40. Chand, N.; Dwivedi, U. K. Polym Compos 2008, 28, 437.